

Enhancing pre-salt 4D monitoring, a deep-water Angolan WATS case study

H. Prigent¹, P. Gourmel¹, A. Rivet¹, M. Gavelle¹, L. Savitskiy¹, C. Beigbeder¹, M. Pouget¹, A. Grandi²

¹ CGG; ² TotalEnergies

Summary

We present a 4D pre-salt reservoir monitoring study from two wide-azimuth towed-streamer (WATS) surveys. Advanced flows were implemented to mitigate complex salt-related challenges and WATS repeatability issues in the image domain. Three models of converted waves interfering at reservoir level were generated via dual salt-flood Kirchhoff demigrations, and then subtracted at the post-migration stage. Repeatability issues were also addressed in the image domain via a novel 4D Least-Squares Wave-Equation Kirchhoff flow. The results reveal an unexpected level of 4D signal in such a complex geological setting.

Enhancing pre-salt 4D monitoring, a deep-water Angolan WATS case study

Introduction

Deep water pre-salt reservoirs bring 4D monitoring to a higher level of complexity and uncertainty. Wide-azimuth streamer surveys specifically designed to illuminate subsalt targets are subject to more repeatability issues than nodal acquisitions. Operating multiple vessels to replicate pre-plot shot and receiver locations is a real acquisition challenge when weather conditions or currents turn adverse. Any azimuthal variation at surface locations will be amplified at reservoir level after propagation through complex salt bodies. Therefore, weak 4D signals stand little chance of being detected below a certain level of shot and receiver repeatability.

The 4D monitoring study presented here is located in deep water offshore Angola. The region features massive salt canopies locally overlying productive reservoir fairways. Two wide-azimuth towed-streamer (WATS) surveys using the Mad Dog design (Saint André et al., 2010) were acquired to optimize illumination at subsalt dipping reservoirs. The Mad Dog design is a multi-vessel and multi-pass deployment, involving one streamer vessel and two source vessels. The acquisition of a survey line is based on the combination of two successive acquisition passes. Clearly, source and receiver repeatability are complex to attain in operations with multiple vessels.

Application of a novel Water Layer Inversion (Dega et al., 2021) allows us to correct for some of the non-repeatable factors during acquisition, such as source position and water velocity. Nonetheless, the combination of the WATS design and salt complexity brings other processing challenges, such as shear-wave attenuation, the preservation of diffractions at regularization stage and pre-salt signal-to-noise enhancement. This abstract will cover the solutions implemented to satisfy these objectives.

Converted waves attenuation in the image domain

Converted waves generated across salt/sediment interfaces become critical in poorly illuminated areas, particularly when they interfere at reservoir level. Generated at strong impedance contrasts, their amplitude can be significantly higher than the P-wave primary signal. Figure 1a describes the three types of converted waves present in our data and their mis-positioning relative to base of salt after migration with P-wave velocity (dotted lines). We model them via a dual-flood Kirchhoff pre-stack demigration scheme (Huang et al., 2013), as illustrated by Figure 1b. All three models are then depth migrated with P-wave velocities (Figure 1c) to perform a 3D joint adaptive subtraction in the image domain, which allows for better dip discrimination between converted waves and primary events, a critical step for preserving weak 4D signal. The flow, which involves many pre-stack demigrations/remigrations, is highly compute-intensive when applied to multiple large fold vintages.

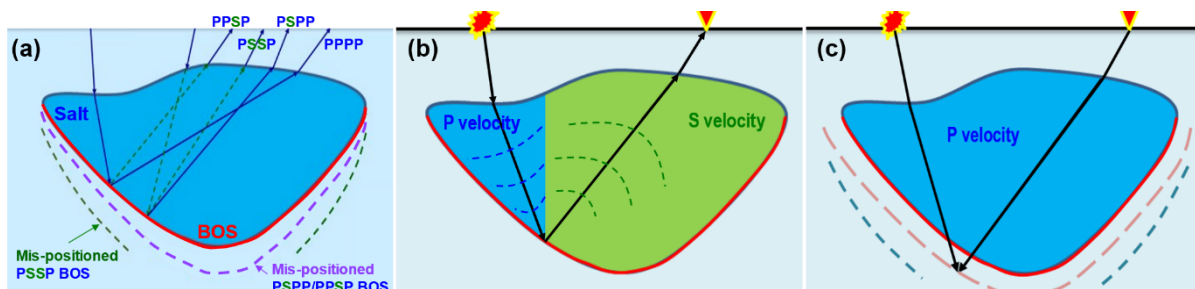


Figure 1 (a) Converted waves present in P-wave PSDM, (b) Dual salt flood modelling, (c) P-wave PSDM of modelled converted waves.

Figure 2 illustrates the results of the attenuation process on the base, monitor and 4D difference. Converted waves are not repeatable between the two vintages and introduce some signal leakage in the 4D difference (Figure 2c), particularly at low frequencies. Their impact on 4D signal is strongly mitigated after application of the correction (Figure 2f).

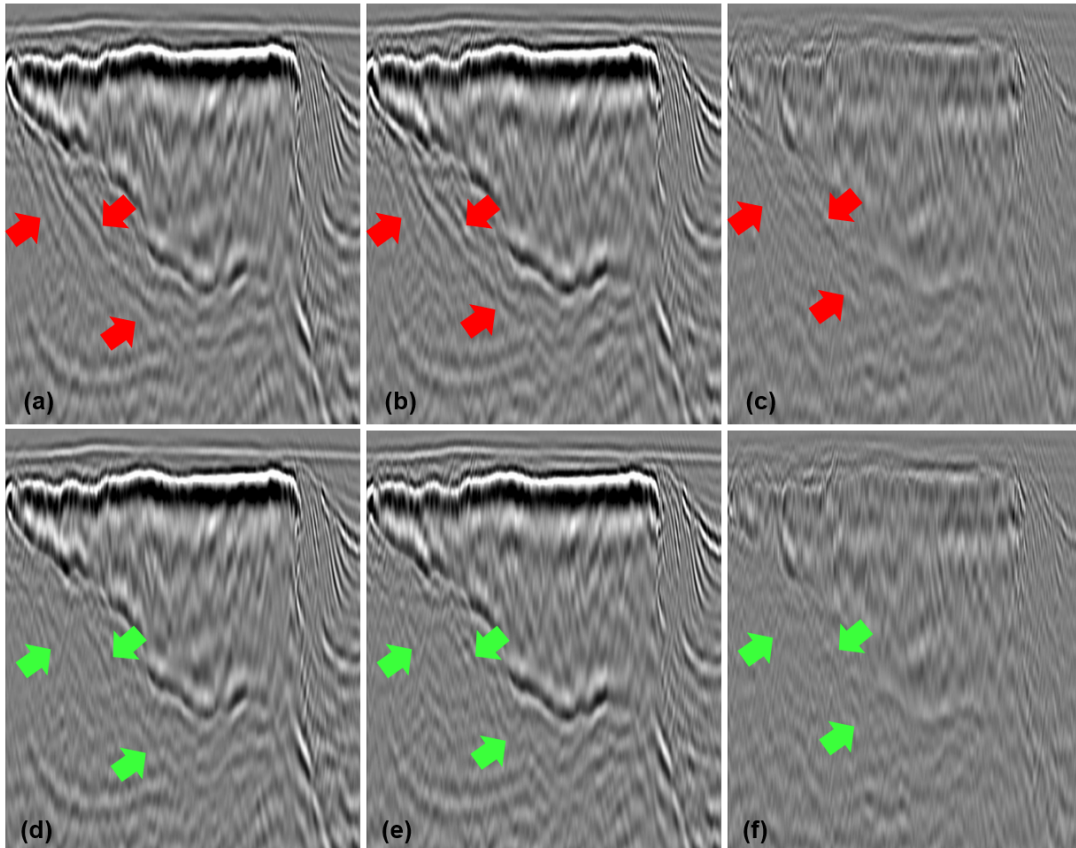


Figure 2 8Hz filtered stacks before and after removal of converted waves: Base before(a)/after(d), Monitor before(b)/after(e) and 4D difference before(c)/after(f).

Image-domain 4D Least-Squares Wave-Equation Kirchhoff flow

The large common offset vector size inherent to WATS acquisition (1000m in crossline offset) makes data domain regularization potentially detrimental to complex diffractions. Traces with significantly different subsurface paths from one bin to another cause strong jitters and unreliable dip estimates for the diffractions. To overcome this issue, we applied a novel image-domain 4D Least-Squares Wave-Equation Kirchhoff migration flow that allows us to avoid data-domain regularization and preserve 4D signal and diffractions (Figure 3).

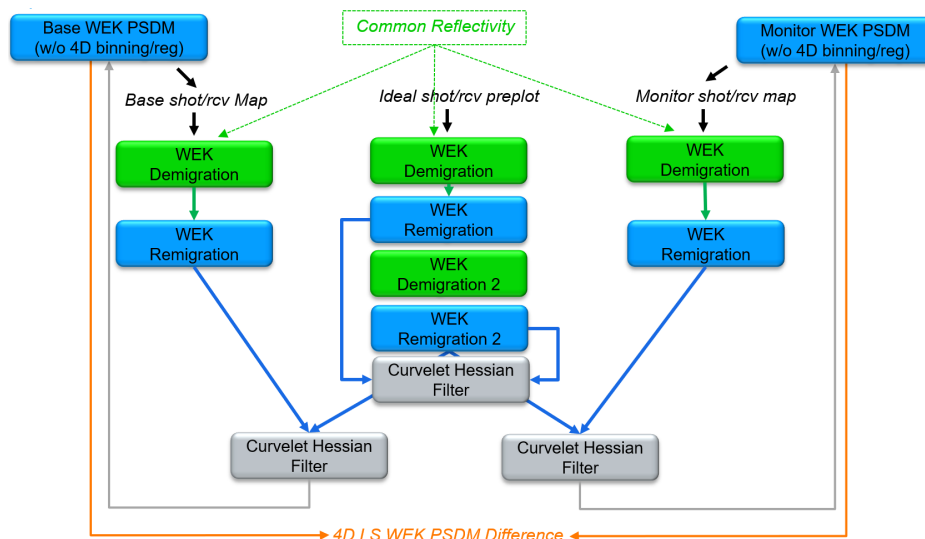


Figure 3 Image-domain 4D Least-Squares Wave-Equation Kirchhoff migration flow

First, we generate the ideal survey grid design, which consists here of perfectly centered offset x and y common offset vectors. We use a common reflectivity cube to generate three auxiliary image cubes by demigration/remigration of the reflectivity model on the ideal grid, on the base acquisition, and on the monitor acquisition geometries. A second demigration/remigration loop is run on the ideal image cube to mitigate geological illumination and migration artifacts. This conventional least-squares imaging loop increases amplitude fidelity and reduces noise in the reference cube, which is used for subsequent 4D matching.

Last, a curvelet domain Hessian filter is calculated separately for the base and the monitor with respect to the ideal image cube. Thus, both base and monitor are converted to an ideal acquisition to efficiently mitigate 4D noise and illumination issues due to non-repeatability. Our 4D least-squares matching flow not only focuses on mitigation of acquisition-related effects (Roodaki et al., 2022) but also accounts for subsalt illumination and migration artifacts thanks to the additional least-squares imaging loop applied to the ideal reference survey.

This flow accommodates either ray-based or wave-equation based migrations and demigrations. In our context, where salt velocity contrasts pose a significant challenge for ray-based travel-time and amplitude computation, we utilized Wave-Equation Kirchhoff (WEK) (Pu et al., 2021) imaging. WEK provides a convenient way to honor complex velocity models. It is superior to ray-based Kirchhoff for sharp velocity contrasts and more affordable than RTM for providing surface-offset gathers. This second advantage becomes crucial when dealing with multiple surveys or wide-azimuth surveys, which is the combination of our 4D example. The uplift from the WEK imaging compared to ray-based Kirchhoff migration is shown in Figure 4. WEK shows better coherence on pre-salt events, as indicated by the green arrows in Figure 4c.

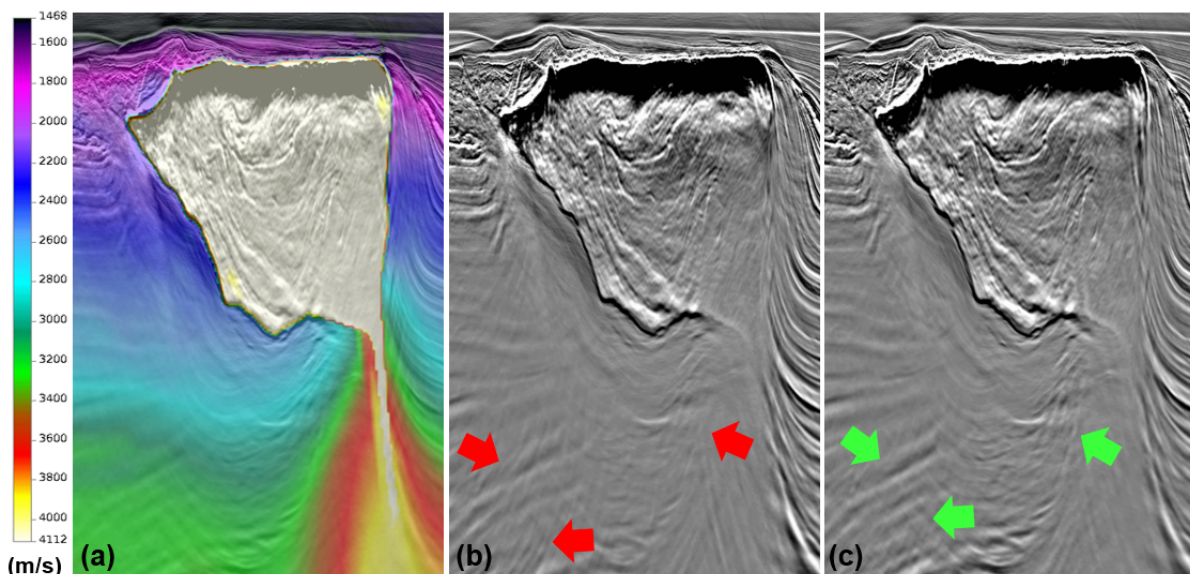


Figure 4 (a) P -wave velocity model, (b) Ray-based Kirchhoff PSDM, (c) WEK PSDM.

Figure 5 compares 4D results of WEK and Least-Squares WEK imaging at subsalt reservoirs. Salt leakage is obviously not removed, but the 4D signal at the reservoirs appears cleaner. The flow reduces 4D noise, as observable within the yellow ellipses, and allows a sharper delineation of the 4D signal, as pointed out by the green arrows.

Both results are displayed after applying a 4D-friendly cooperative noise attenuation step in the complex wavelet transform domain (Peng and Huang, 2014). This process helped in further eliminating migration artifacts from the WEK image. Given the already lower noise level on the corresponding Least-Squares WEK image, a much milder version of this denoise step could be applied with the new flow, thus reducing the risk of 4D signal leakage.

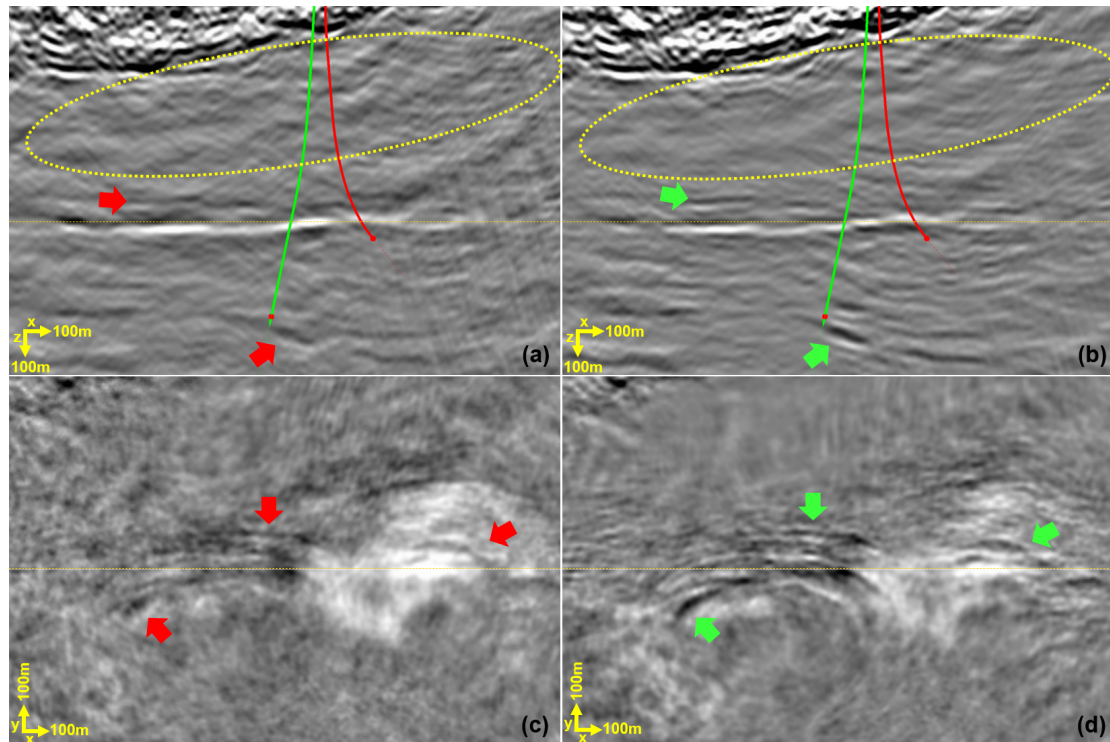


Figure 5 4D difference stacks in section (top) and depth slice (bottom) views at reservoirs: WEK (a,b) and Least-Squares WEK (b,d)

Conclusions

This case study is an original example of subsalt monitoring from WATS data. We have implemented innovative workflows to mitigate the challenges related to the presence of complex salt bodies in a 4D compatible way. The full processing delivered an unexpected level of 4D signal over the deep pre-salt reservoir. We demonstrated the feasibility of large-scale subsalt reservoir monitoring with WATS surveys, a more cost-effective solution than nodal acquisitions. Future focus on refining velocity models with elastic FWI or 4D FWI could further improve our image domain flows.

Acknowledgements

The authors thank TotalEnergies, their partners and ANPG for permission to show the data examples.

References

- Dega, S., Allemand, T., Yu, Z., Salaun, N., Lafram, A. and Grandi, A. [2021] Revealing 4D subsidence with a 3D water-bottom travel times inversion. *81st EAGE Conference & Exhibition*, Extended Abstracts.
- Huang, Y., Gou, W., Leblanc, O., Li, Y., Ji, S. and Huang, Y. [2013] Study and Application of Salt-Related Converted Waves in Imaging. *83rd Annual International Meeting, SEG*, Expanded Abstracts, 3851-3855.
- Peng, C. and Huang, R. [2014] Cooperative Noise Attenuation in a Complex Wavelet Transform Domain. *76th EAGE Conference & Exhibition*, Extended Abstracts, Th ELI1 03.
- Pu, Y., Liu, G., Wang, D., Huang, H. and Wang, P. [2021] Wave-equation travelttime and amplitude for Kirchhoff migration. *1st International Meeting for Applied Geoscience & Energy*, SEG, Expanded Abstracts, 2684-2688.
- Roodaki, A., Papillon, F., Prigent, H., Yu, Z., Mahgoub, M. and Cambois, G. [2022] Enhanced 4D signal via 4D Least-Squares Migration when repeatability is not guaranteed. *SEG workshop on Multiple Approaches to Time-lapse Monitoring for Carbonate Reservoirs, Abu Dhabi*.
- Saint André, C., Khaled, N., Bovet, L., Brittan, J., Bekara, M., Martin, T. and Phillips, M. [2010] Angola wide azimuth towed streamer (WATS): 3-D SRME whilst shooting. *80th Annual International Meeting, SEG*, Expanded Abstracts, 3416-3420.